BULLETIN OF THE POLISH ACADEMY OF SCIENCES
TECHNICAL SCIENCES, Vol. 72(3), 2024, Article number: e149814
DOI: 10.24425/bpasts.2024.149814

The use of computed tomography and scanning microscopy methods for assessing the alkaline reactivity of aggregate

Justyna ZAPAŁA-SŁAWETA*

Faculty of Civil Engineering and Architecture, Kielce University of Technology, Al. Tysiąclecia Państwa Polskiego 7, 25-314 Kielce, Poland

Abstract. The reaction of alkalis with aggregate containing reactive forms of silica (ASR) plays a significant role in shaping the durability of concrete, as the strongly hygroscopic reaction products generated lead to internal stress, causing its expansion and cracking. This study presents an extended analysis of corrosive processes occurring in mortars with reactive natural aggregate from Poland, using computed tomography and scanning microscopy methods. Numerous cracks in the grains and the surrounding cementitious matrix were observed, indicating a high degree of advancement of corrosive processes. Over time, the proportion of pores with reduced sphericity increased, indicating ongoing degradation of the mortars. The usefulness of computed tomography in studying the progress of ASR was demonstrated. Scanning microscopy confirmed that the cause of mortar degradation is the formed ASR gel with a typical composition, located within the volume of reactive grains, cracks propagating into the cementitious matrix, and accumulated in air voids.

Keywords: alkali-silica-reaction; microstructure degradation; computed tomography; SEM-EDS.

1. INTRODUCTION

One of the reasons for the reduced durability of concrete is internal corrosion caused by the reaction of metastable forms of silica in the aggregate with a strongly alkaline solution in the pores of the concrete. The reaction products are sodium-potassium-calcium silicate gels, which, by absorbing moisture, swell, inducing stress in the aggregate and the surrounding cementitious matrix, leading to significant expansion and cracking of the concrete [1].

ASR involves several successive reactions: the dissolution of metastable silica forms, the formation of nanocolloidal silica sol, sol gelation, and gel swelling [2]. The kinetics of ASR are mainly dependent on the solubility of silica, which, in turn, depends on the mineral composition of the aggregate, the content, and form of reactive silica in the aggregate, aggregate texture, grain size, surface properties, the composition of the solution in the concrete pores, temperature. The stability of silica in an alkaline solution decreases with an increase in the degree of defectiveness of its network and a decrease in crystallinity. Therefore, the reactivity of minerals increases in the following order: silica containing structural defects <metastable silica (cristobalite, tridymite) <cryptocrystalline silica and fibrous silica (chalcedony) < amorphous silica (opal, volcanic glass, synthetic glass) [3, 4]. Aggregate is considered potentially reactive when the threshold content of reactive components is exceeded. It has been indicated that fine and coarse aggregates exhibit potential reactivity with alkalis when the contents of reactive minerals exceed, respectively: 0.5% – opal, 1% – tridymite, cristobalite, 3.0% – chert or chalcedony, natural volcanic glass, 5.0% – microcrystalline quartz, strained quartz [5–7]. When evaluating the reactivity of aggregate, the texture of the rock and the type of constituent minerals should also be considered. Coarse-grained rocks are believed to be more reactive with alkalis due to significant microstructure cracking compared to fine-grained rocks. The type of rock binder also plays a significant role. Crystalline or lithographic limestone, which is typically inert, can be reactive if it contains silica or clay minerals dispersed in the matrix [8].

Numerous studies of aggregate reactions with alkalis indicate different reaction pathways. Some aggregates react superficially, while others only within internal microcracks and defects [9–11]. Significant importance is attributed to the availability of alkaline pore solution to reactive silica. If the aggregate is entirely composed of reactive silica, as in the case of volcanic glass, or opal, the aggregate surface reacts with alkalis, creating a dense layer of ASR gel, visible as a reaction rim. However, if reactive silica is dispersed in a non-reactive aggregate matrix, the gel forms within the aggregate and the reaction rate depends on the availability of pore solution to reactive silica, facilitated by existing microcracks inside the aggregate [12, 13]. A different course of the reaction was observed in the case of aggregates containing reactive silica as a cementitious component bonding fine, non-reactive quartz grains, indicating that the reactive rim forms from liberated quartz grains in the matrix and partially precipitated silica at the aggregate-cement paste interface. The reactive rim at the contact zone between the aggregate and the cement paste or within the grain limits the escape of ASR gels formed within the grain, leading to grain swelling [14]. The mul-

*e-mail: jzapala@tu.kielce.pl

Manuscript submitted 2023-10-18, revised 2024-01-17, initially accepted for publication 2024-02-18, published in May 2024.

© 2024 The Author(s). This is an open access article under the CC BY license (http://creativecommons.org/licenses/by/4.0/)

titude of factors influencing the course of alkali-aggregate reactions underscores the complexity of these processes and the need for further analysis.

A common method for determining whether aggregate is potentially reactive is to test the expansion of mortars and concrete made from this aggregate. To assess the degree of microstructure damage and confirm the formation of swelling ASR gels, SEM-EDS analysis is performed. The microscopic method requires the sampling and preparation of a specimen in the form of a fracture or polished section, and real-time observation of corrosive processes is challenging but possible. A much simpler non-destructive method for observing changes in the material microstructure is computed tomography. Computed tomography is a non-destructive method that allows for obtaining and analysing the internal structure of the material. The creation of a tomographic image involves measuring the absorption of radiation passing through the object. The method utilizes a combination of object projections taken from various directions to create cross-sectional and volumetric images [15]. It also provides valuable information, such as porosity, pore geometry, and pore tortuosity, which, when analysed during the reaction, indirectly indicate the degree of advancement of corrosive processes.

This study presents the results of research on the course of corrosive processes induced by the reaction of natural polymineral glacial gravel aggregate with alkalis. Observations of changes in the microstructure of mortars during their exposure to corrosive factors were made using computed tomography. The obtained results were related to the linear expansion of mortars over time and the observation of the microstructure under a scanning electron microscope. Based on the obtained research results, a likely course of corrosive processes due to the reaction of polymineral aggregate with alkalis was proposed.

2. MATERIALS AND METHODS

2.1. Materials and mix proportion

In the research, natural polymineral gravel aggregate from the northern regions of Poland was used. The mineral composition of the aggregate is presented in Fig. 1. Table 1 provides a petrographic analysis of the aggregate, indicating components exhibiting potential reactivity with alkalis.

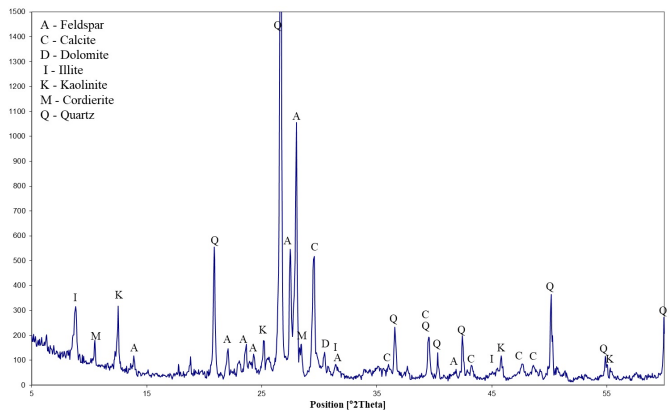

Fig. 1. XRD diffraction pattern of gravel aggregate [17]

Table 1
Petrographic analysis of the aggregate [16, 17]

Rock type	Content [%]	Reactive mineral component
Organo-dendritic, sparite-micrite limestone	28.0	Cryptocrystalline quartz
Quartz-glaukonite sandstone	13.8	Chalcedony, microcrystalline quartz
Feldspar-biotite granite	10.5	Strained quartz
Metamorphous quartz-pyroxene shale with opal	3.9	Opal cement
Unreactive component	43.8	–

To determine the potential reactivity of the aggregate, the methodology outlined in ASTM C1260 was employed, which is an accelerated method for assessing aggregate reactivity using mortar bars [18]. Portland cement CEM I 42.5 R was used with a total alkali content of Na_2O_e = 0.71% and a chemical composition as presented in Table 2. The aggregate-to-cement ratio was 2.25:1, with a w/c ratio of 0.47. The natural aggregate constituted 100% of the aggregate blend, and its particle size distribution was adjusted to meet the requirements of ASTM C1260 by mechanically reducing the fraction by 4–16 mm. To evaluate changes in the microstructure of mortars using computed tomography, mortars with the same composition as these intended for expansion testing were prepared.

2.2. Test methods

The potential reactivity of the aggregate was assessed following the methodology outlined in ASTM C1260. After 24 hours of curing, the mortar bars were demoulded and then stored for an additional 24 hours in water at a temperature of 80°C. Following this, a so-called zero measurement of the length of the samples was performed using a Graff-Kauffmann apparatus (accuracy of 0.005 mm). Subsequently, the mortar bars were placed in a 1M NaOH solution at 80°C and stored for 28 days. Length measurements of the mortar bars were taken daily for the first 14 days and then at seven-day intervals. The expansion of the mortars was determined as the average of the length measurements of three mortar bars.

Samples from the mortars in which corrosive processes were observed using computed tomography were stored under the same conditions as the mortar bars intended for linear change testing. The initial observations were made after 24 hours of mortar storage in water at 80°C, followed by observations at 3, 7, 14, 21, and 28 days of immersion in the 1M NaOH solution. The research was conducted using a Nikon XT H 225 ST computed tomography scanner. The tomograph is equipped with an X-ray tube generating radiation at a maximum voltage of 225 kV and a power of 450 W. Scans were performed at a voltage of 220 kV and a current intensity of 77 µA. These values were experimentally determined through multiple scans of the sample to obtain the best parameters for the material being studied. For each sample, 4500 2D images were acquired, with an exposure

Table 2
Cement chemical composition [%]

Material	SiO_2	Al_2O_3	Fe_2O_3	CaO	MgO	SO_3	K_2O	Na_2O	TiO_2	LOI*	N.s.p.**
Cement	20.26	4.69	2.33	62.29	2.15	3.03	0.80	0.18	0.45	2.45	0.99

time of 250 µs for each image. After compiling the 2D images, a three-dimensional model with a voxel resolution of 14 µm for each sample was created using the CT Pro 3D software. Subsequently, the 3D model was analysed using VG Studio Max 3.4 software.

The impact of corrosive processes on the microstructure of mortars with reactive aggregate was examined on polished mortar samples, and observations were made under a scanning electron microscope (FEI COMPANY QUANTA FEG 205). Samples were taken after 28 days of exposure to corrosive conditions and prepared by their sectioning from the central part of mortar bars using a slow-speed diamond saw followed by grinding and polishing the surface on a diamond suspension. Observations were conducted in backscattered electron (BSE) mode at a voltage of 15 keV. The energy dispersive X-ray analysis (EDAX) allowed for elemental composition determination in micro-areas. No conductive coating was applied to the samples.

3. RESULT

3.1. Expansion results

In Fig. 2, the results of mortar expansion, tested using the accelerated method in accordance with ASTM C1260, are presented.

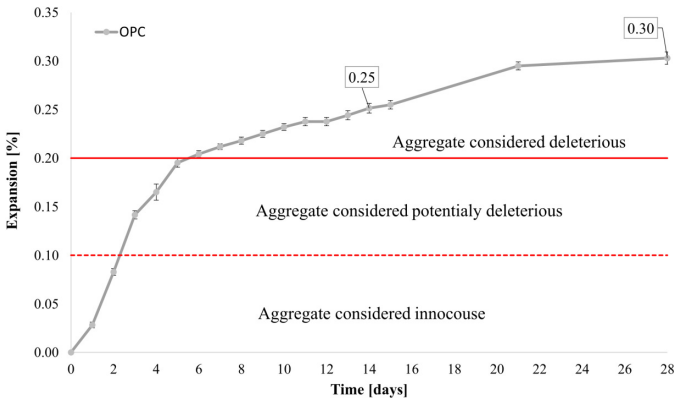

Fig. 2. Expansion behaviour of the mortar bars containing mechanically crushed gravel aggregate

The values of linear expansion of the samples indicate that the aggregate tested reacts with alkalis and can lead to mortar degradation. The threshold indicating potential aggregate reactivity, which is 0.1%, was exceeded as early as the third day of the test (dashed red line), while the threshold classifying the aggregate as reactive, which is 0.2%, was reached on the sixth day of the test (solid red line).

Mortar expansion after 14 days reached a value of 0.25% and increased by 20% to a value of 0.30%. The expansion curve indicates a rapid reaction of the aggregate with alkalis, and the observed expansion value after 14 days classifies it as having moderate reactivity [19].

3.2. Mortar microstructure

In Fig. 3, selected cross-sections in the form of 2D images of the mortars after 0, 3, 7, 14, 21, and 28 days of immersion in the 1M NaOH solution are presented. In the tomographic

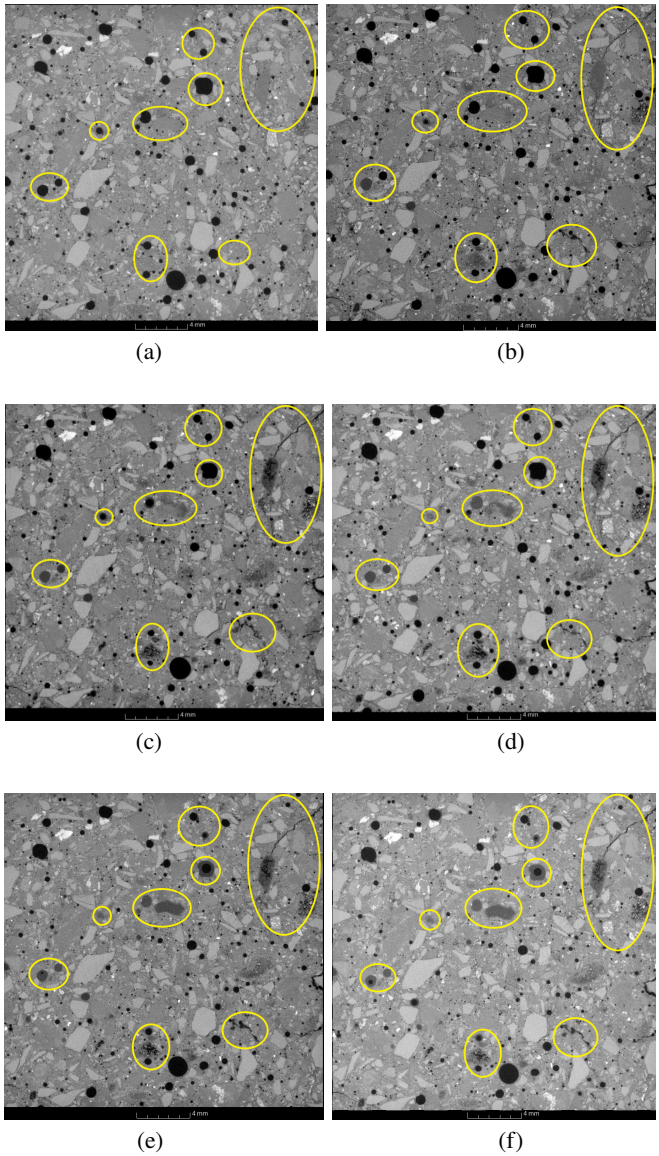

Fig. 3. 2D images obtained by X-ray µCT of gravel aggregate mortars stored in 1M NaOH after a) 0 days, b) 3 days, c) 7 days, d) 14 days, e) 21 days, f) 28 days. Corrosion centers and air voids gradually filled with gel were marked in yellow

images, each shade of grey corresponds to objects with a specific density and atomic mass [20]. Objects appearing brighter have higher density, while darker areas correspond to materials with lower density and atomic mass. Air voids, which do not absorb X-rays, are visible as dark areas, while the aggregate grains and cement paste appear as brighter areas with varying shades of grey.

A few primary or secondary cracks in the aggregate grains are visible, which may have formed during the mechanical reduction of coarse fractions. Over time, during exposure to corrosive conditions, gradual over-reaction of the reactive aggregate grains with alkalis was observed, and the rate of reaction of the grains varied. Swelling reaction products formed in the grains, as evidenced by the visible cracks, dark areas within the reacting grains, and cracks propagating into the cement paste. With time, the degree of degradation of the aggregate grains and the number of cracks in the cementitious matrix increased, and these cracks were partially filled with ASR gels to varying extents.

Accumulation of solid ASR products, possibly gels, in some air voids was also observed. In the computed tomography images, even after three days, partial filling of some voids with reaction products was observed. After 21 and 28 days, some of the voids were completely filled. The crack in the microstructure of the mortars with reactive aggregate confirms that the ongoing reaction leads to the generation of swelling pressure, resulting in mortar expansion.

A notable advantage of computed tomography is the ability to monitor in-situ changes occurring in the microstructure of mortars, including changes in pore sizes and shapes [21]. In the graph presented in Fig. 4, the relationship between pore sphericity and their diameter is shown. Sphericity is a parameter that characterises the shape of pores, indicating how closely the shape of an object matches that of a sphere using an appropriate volume-to-surface ratio. The maximum sphericity value can

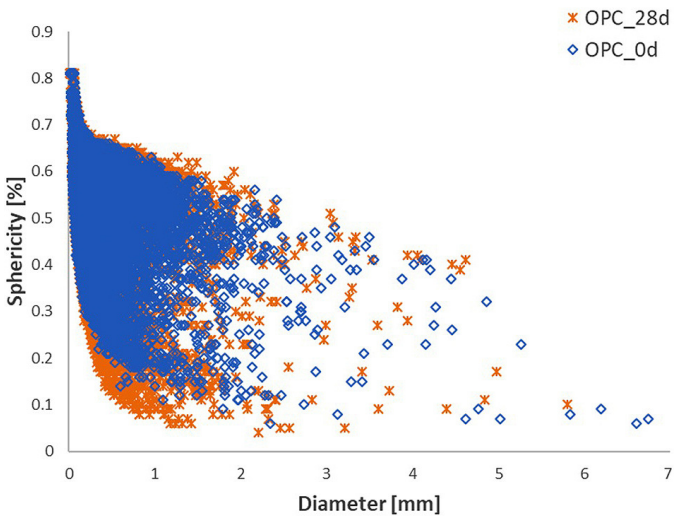

Fig. 4. Dependence of pore sphericity on diameter in mortars after 0 and 28 days of the test

be 1, which means a spherical shape, while the minimum is 0. The relationship between pore shape and dimensions, analysed alongside ASR progression, can provide a more comprehensive understanding of the changes occurring in the sample. The gel, exerting pressure on the walls of cement paste pores, leads to crack formation [22]. Some pores may connect with cracks formed due to ASR, increasing pore dimensions in a specific direction and thus reducing their sphericity, as indicated in previous research by Yang *et al.* [21]. To assess the extent of reaction in the studied mortars, the characterisation of the voids/pores was conducted. Due to limited resolution, the analysis does not cover gel porosity or capillary porosity but focuses on pores with a diameter greater than 14 μm. The analysis allows for the observation of changes induced by ASR. For better clarity of the occurring changes, the results after 0 and 28 days of exposure to corrosive conditions were compared.

A decrease in pore sphericity is visible after 28 days of exposure to corrosive conditions compared to the zero measurements. The increase in the content of non-spherical voids is associated with the formation of cracks caused by the swelling of the ASR gel.

As shown in the tomographic images, some small cracks were filled with gel, while larger cracks remained empty. It is also likely that the increase in the content of non-spherical voids with a diameter of up to 1 mm results from the degradation of the reactive aggregate grains themselves, which, as a result of advanced reaction with alkalis, leave empty spaces. Because some cracks formed due to the stress generated by reacting grains are filled with reaction products, there is no observable increase in the content of elongated, and voids with little sphericity.

To further understand the changes in the microstructure of the mortar observed in tomographic studies, observations were made under a scanning electron microscope. These studies aimed to precisely locate and identify ASR products through micro-area analysis. These observations were made after 28 days of immersion of the samples in the NaOH solution. Images depicting the degraded microstructure of the mortar are presented in Fig. 5.

Scanning electron microscope observations of mortars with reactive aggregate confirmed numerous corrosion centres and significant degradation of the mortars. Cracks in the grains, partially filled with reaction products, were observed (Fig. 5a), propagating into the cement paste. Corrosion centres were observed as well as cracks filled with ASR gel, penetrating the grain and moving into the cement paste.

Clusters of gels that completely replaced the volume of the grain or filled pores in the cement paste were also present (Fig. 5b, d). Relics of strongly corroded aggregate grains were also observed (Fig. 5c). The accumulation of highly hydrated products in air voids located in the cement paste was confirmed.

EDS analysis of the formed products indicated that they are sodium-potassium-calcium silicates with different compositions (items 1–3). Products located in the cement paste (item 2) and in the air void (item 4) showed an increased calcium content, whose main source was calcium hydroxide and the C-S-H phase [23].

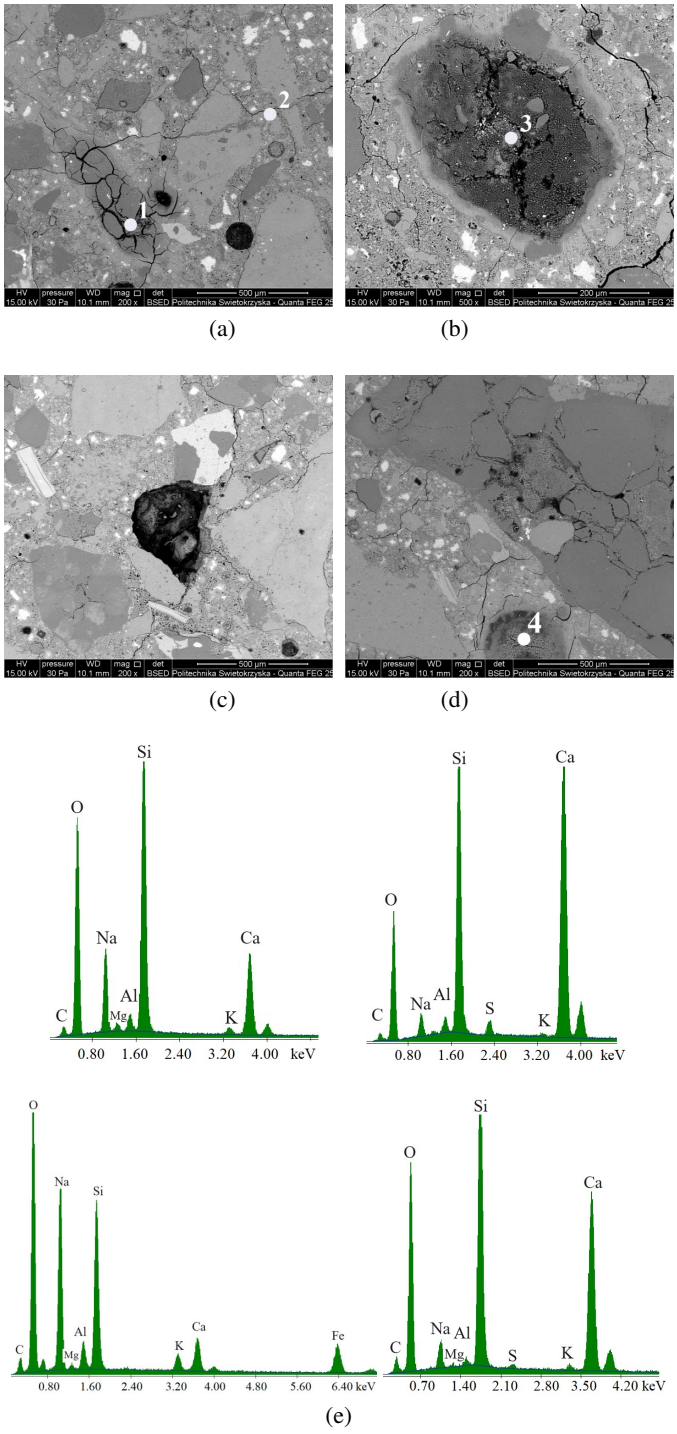

Fig. 5. Microstructure images of the mortar depicting: a–b) cracked reactive aggregate grains, c) aggregate relic, d) air void filled with ASR, e) X-ray microanalysis at points 1–4

4. DISCUSSION

The damage detected by computed tomography in mortars with crushed gravel aggregate confirms that the aggregate exhibits harmful reactivity with alkalis. Due to the diverse petrographic composition, individual rocks may react differently. As a result of the reaction in some grains, products are formed throughout the entire volume of the grain, exerting stress on the surrounding cement paste. This leads to the formation of micro-cracks in the paste. Other grains react primarily on the surface, and the corrosion processes occur more slowly. Gel accumulates in air voids after only three days of reaction and partially fills them, indicating that the gel is liquid, and the reaction of silica with alkalis occurs rapidly. At lower temperatures, the solution in the pores becomes saturated with respect to $Ca(OH)_2$, reducing the solubility of silica. At higher temperatures and with access to alkalis from an external source, the decreased concentration of Ca^{2+} ions increases the concentration of OH^- ions, which attack the silanol and siloxane groups of silica [24, 25]. Tomographic images taken after seven days indicate significant progress in the reaction of the aggregate with alkalis. Cracks in the reactive grain and empty areas indicative of grain degradation are visible. The reaction continues until the reactive material is exhausted, and weakened grains no longer generate pressure on the cement paste, causing it to crack [26]. Further observations showed the filling of some air voids with reaction products. Numerous cracks in the cement matrix were also filled with ASR gels. The observations of changes in the mortar microstructure during the test are consistent with measurable effects of the reaction, such as mortar expansion. The greater the degradation of reactive grains and the cement paste, the higher the values of measurable expansion.

Observations of the microstructure under a scanning electron microscope confirm different reactions in individual grains with varying compositions. The aggregate grains exhibit different reactivity and susceptibility to cracking, resulting in varying degrees of destruction of both the grain itself and the surrounding cement paste. Additionally, gels with different compositions formed in the grain generate different swelling pressures. The gels filling the cracks generate pressure on the cement paste, and their mechanical properties are responsible for further measurable expansion [27]. Based on the tomographic studies, it was indicated that the kinetics of the reaction of gravel aggregate with alkalis vary due to differences in mineral composition, content, and availability of reactive silica. In the case of slow-reacting or poorly reactive aggregates, ASR gels may mainly accumulate in the grains without transferring to the cement paste, as supported by the existing literature reports. On the other hand, rapidly reacting aggregates produce large amounts of gels that propagate into the cement paste and air voids [28].

The mechanism of degradation of the reactive grain and cement paste depends on the initiating mechanism of cracking. For quickly reacting, homogeneous aggregate grains, a reaction envelope is formed, and the crack pattern corresponds to the cracking of successive layers (called onion skin cracking), initially observed in the interfacial transition zone between the aggregate and the cement paste. Slow to moderately reacting, heterogeneous aggregates crack in reactive zones, and the areas of gel formed (gel pockets) create pressure within the grain volume, leading to the formation of sharp cracks [26,29]. Expansion models depend on the homogeneity of the aggregate [30]. In aggregates of average homogeneity, a combination of cracking patterns occurs. Based on the conducted research, gravel aggregate can be classified as heterogeneous aggregates with varying degrees of reactivity due to their diverse mineral composition,

different content of reactive components, possibility of diffusion of OH^-, Na^+, K^+, and Ca^{2+} ions to the reactive zones. The varied composition of ASR gels formed in differently reacting grains is also of significance.

5. CONCLUSIONS

This work presents the progression of corrosive processes induced by the reaction of polymineral glacial gravel aggregate with alkalis using computed tomography and scanning electron microscopy. Computed tomography is an effective and non-destructive research method that allows monitoring of the course of corrosive processes in situ. Scanning electron microscopy (SEM) and the energy dispersive X-ray allows for confirmation of the causes of mortar destruction by analysing the microstructure and composition of the resulting products.

The obtained results were compared with the recorded changes in the linear elongation of mortar bars.

Based on the observations and discussion of the results, the following conclusions were drawn:

- The computer tomography method can be used as a tool for continuous monitoring of phenomena occurring during the alkali-aggregate reaction. The degree of degradation of mortars due to ASR is reflected in the measurable expansion of mortar bars.
- The kinetics of the reaction of the aggregate with alkalis vary for different types of reactive grains. Quickly reacting aggregate generates significant stress on the surrounding cement paste, causing it to crack. The rapid expansion of the mortar in the initial stages is attributed to the cracking in both the reactive grains and the cement paste matrix. Further expansion can be driven by additional cracking in the cement paste. Surface-reacting aggregates degrade more slowly and likely contribute to a slow, gradual increase in mortar expansion. The reaction of the aggregate with alkalis occurs continuously until the reactive components in the aggregate are depleted.
- ASR gels accumulate in air voids, indicating a high degree of reaction even in the early stages. Some air voids are completely filled with reaction products, while others are only partially filled. The presence of air voids provides additional free spaces for the formed ASR gels and may reduce the degree of mortar degradation. However, reaction products in air voids that are completely filled likely exert stress on the cement paste.
- ASR gels exhibit varying swelling abilities due to differences in chemical composition. Gels formed within the aggregate have low calcium content and high sodium and potassium content. The farther from the aggregate, the higher the calcium content and the limited ability to swell.
- The gravel aggregate was classified as moderately reactive due to its polymineral nature and varying degrees of heterogeneity. Grains containing different forms of reactive silica dispersed within the aggregate matrix react differently, resulting in diverse patterns of cracking in both the aggregate and the matrix.

REFERENCES

[1] T.E. Stanton, "Influence of cement and aggregate on concrete expansion," *Eng. News-Rec.*, vol. 124, pp. 171–173, 1940.

[2] F. Rajabipour, E. Giannini, C. Dunant, J.H. Ideker, M.D.A. Thomas, "Alkali–silica reaction: Current understanding of the reaction mechanisms and the knowledge gaps," *Cem. Concr. Res.,* vol. 76, pp. 130–146, 2015, doi: 10.1016/j.cemconres.2015.05.024.

[3] A.B. Poole, "Introduction to alkali–aggregate reaction in concrete," in: *The Alkali Silica Reaction in Concrete*, R.N. Swamy (Ed.), Van Nostrand Reinhold, New York, 1992.

[4] M.A.T.M. Broekmans, "Structural properties of quartz and their potential role for ASR," *Mater. Charact.*, vol. 53, no 2–4, pp. 129–140, 2004, doi: 10.1016/j.matchar.2004.08.010.

[5] R.C. Mielenz, "Petrographic examination (Mineral aggregates)," *ASTM STP 169B*, pp. 539–572, 1978.

[6] L.M. Dolar, *Handbook of concrete aggregates: A petrographic and technological evaluation*. Noyes Publications: Park Ridge, N.J. p. 345, 1983.

[7] NRMCA "Guide specifications for concrete subject to alkali-silica reactions," Mid-Atlantic Regional Technical Committee, (Available through NRMCA, Silver Spring, Maryland), 1993.

[8] M. Ratnam, *Monograph on Alkali Aggregate Reaction.* Central Soil & Materials Research Station, New Delhi, 2008.

[9] J. Zapała-Sławeta and Z. Owsiak, "Effect of lithium nitrate on the reaction between opal aggregate and sodium and potassium hydroxides in concrete over a long period of time," *Bull. Pol. Acad. Sci. Tech. Sci.*, vol. 65, no. 6, pp. 773–778, 2017, doi: 10.1515/bpasts-2017-0085.

[10] H. Maraghechi, S. Shafaatian, G. Fischer, and F. Rajabipour, "The role of residual cracks on alkali silica reactivity of recycled glass aggregates," *Cem. Concr. Compos.*, vol. 34, pp. 41–47, 2012, doi: 10.1016/j.cemconcomp.2011.07.004.

[11] Z. Owsiak, J. Zapała-Sławeta, and P. Czapik, "Diagnosis of concrete structures distress due to alkali-aggregate reaction," *Bull. Pol. Acad. Sci. Tech. Sci.*, vol. 63, no 1, pp. 23-29, 2015, doi: 10.1515/bpasts-2015-0003.

[12] E.R. Gallyamov, A. Leemann, B. Lothenbach, and J.-F. Molinari, "Predicting damage in aggregates due to the volume increase of the alkali-silica reaction products," *Cem. Concr. Res.*, vol. 154, p. 106744, 2022, doi: doi: 10.1016/j.cemconres.2022.106744.

[13] M. Shakoorioskooie, M. Griffa, A. Leemann, R. Zboray, and P. Lura, "Alkali-silica reaction products and cracks: X-ray microtomography-based analysis of their spatial-temporal evolution at a mesoscale," *Cem. Concr. Res.*, vol. 150, p. 106593, 2021, doi: 10.1016/j.cemconres.2021.106593.

[14] P. Rivard, J.-P. Ollivier, and G. Ballivy, "Characterization of the ASR rim Application to the Potsdam sandstone," *Cem. Concr. Res.*, vol. 32, pp. 1259–1267, 2002, doi: 10.1016/S0008-8846(02)00765-2.

[15] E. Ratajczyk, "Tomografia komputerowa CT w zastosowaniach przemysłowych. Cz. I Idea pomiarów, główne zespoły i ich funkcje," *Mechanik*, vol. 84, no. 2, pp. 111–117, 2011.

[16] P. Czapik, "Degradation of Glaukonite Sandstone as a Result of Alkali-Silica Reactions in Cement Mortar," *Materials*, vol. 11, no. 6, p. 924, 2018.

[17] J. Zapała-Sławeta and Z. Owsiak, "The role of lithium compounds in mitigating alkali-gravel aggregate reaction," *Constr.*

Build. Mater., vol. 115, pp. 299–303, 2016, doi: 10.1016/j.conbuildmat.2016.04.058.

[18] ASTM C1260–14, Standard Test Method for Potential Reactivity of Aggregates (Mortar-Bar Method). ASTM International: West Conshohocken, PA, USA, 2014.

[19] Z. Giergiczny *et al.*, *Wytyczne techniczne klasyfikacji kruszyw krajowych i zapobiegania reakcji alkalicznej w betonie stosowanym w nawierzchniach dróg i drogowych obiektach inżynierskich. Nowelizacja v2*, 2022. [Online] Available: https://www.gov.pl/attachment/15a40897-941a-4127-8bbe-959c04e97a27

[20] S. Kamalian, M.H. Lev, and R. Gupta, "Computed tomography imaging and angiography – principles," *Handb. Clin. Neurol.*, vol. 135, pp. 3–20, 2016, doi: 10.1016/B978-0-444-53485-9.00001-5.

[21] M. Yang, S.R. Paudel, and E. Asa, "Comparison of pore structure in alkali activated fly ash geopolymer and ordinary concrete due to alkali-silica reaction using micro-computed tomography," *Constr. Build. Mater.*, vol. 236, p. 117524, 2020, doi: 10.1016/j.conbuildmat.2019.117524.

[22] T. Ichikawa, "Alkali silica reaction, pessimum effects and pozzolanic effect," *Cem. Concr. Res.,* vol. 39, pp. 716–726, 2009, doi: 10.1016/j.cemconres.2009.06.004.

[23] M. Regourd-Moranville, "Products of reaction and petrography examination," in *Proc. 8th ICAAR*, K. Okada, Ed., Kyoto, 1989, pp. 445–456.

[24] H. Maraghechi, F. Rajabipour, C.G. Pantano, and WD. Burgos, "Effect of calcium on dissolution and precipitation reactions of amorphous silica at high alkalinity," *Cem. Concr. Res.*, vol. 87, pp. 1–13, 2016, doi: 10.1016/j.cemconres.2016.05.004.

[25] J. Kleib *et al.*, "The use of calcium sulfoaluminate cement to mitigate the alkali silica reaction in mortars," *Constr. Build. Mater.,* vol. 184, pp. 295–303, doi: 10.1016/j.conbuildmat.2018.06.215.

[26] C.F. Dunant, and K.L.Scrivener, "Effects of aggregate size on alkali-silica-reaction induced expansion," *Cem. Concr. Res.*, vol. 42, pp. 745–751, 2012, doi: 10.1016/j.cemconres.2012.02.012.

[27] H.E. Vivian, "The mechanism of alkali-aggregate reaction in concrete," in *Proc. 9th ICAAR*, A.B. Poole, Ed., London, 1992, pp. 1085–1089,

[28] R.F. Bleszynski and M.D.A. Thomas, "Microstructural studies of alkali-silica reaction in fly ash concrete immersed in alkaline solutions," *Adv. Cem. Based Mater.*, vol. 7, pp. 66–78, 1998, doi: 10.1016/S1065-7355(97)00030-8.

[29] T. Miura, S. Multon, and Y. Kawabata, "Influence of the distribution of expansive sites in aggregates on microscopic damage caused by alkali-silica reaction: Insights into the mechanical origin of expansion," *Cem. Concr. Res.,* vol. 142, p. 106355, 2021, doi: 10.1016/j.cemconres.2021.106355.

[30] Z. Owsiak, P. Czapik, J. Zapała-Sławeta, "Methods of mitigating alkali reactvity of gravel aggregate," *Struct. Environ.*, vol. 14, no. 3, pp. 102–109, doi: 10.30540/sae-2022-013.